Effect of Friction Model on Simulation of Hydraulic Actuator

Hideki YANADA*[1], War Htun KHAING*[2], and Xuan Bo TRAN*[3]

*1 Department of Mechanical Engineering, Toyohashi University of Technology
1-1 Hibarigaoka, Tempaku-cho, Toyohashi 441-8580, JAPAN
yanada@me.tut.ac.jp

*2 Department of Mechanical Engineering, Toyohashi University of Technology
1-1 Hibarigaoka, Tempaku-cho, Toyohashi 441-8580, JAPAN
starvilla.85@gmail.com

*3 Department of Fluid Power & Automation Engineering
School of Transportation Engineering, Hanoi University of Science and Technology
C6-205, No.1, Dai Co Viet, Hai Ba Trung, Hanoi, VIETNAM
bo.tranxuan@hust.edu.vn

Abstract

This paper examines the effect of friction model on the simulation accuracy of a hydraulic cylinder by using three friction models: a steady-state friction model, the LuGre model, and the new modified LuGre model. Hydraulic cylinder's behaviors were measured under sinusoidal input to the servo valve. Simulations were conducted under the same conditions as the experiments. The comparisons of simulated results with measured ones show that the new modified LuGre model can predict accurately the hydraulic cylinder's behaviors. Meanwhile, the steady-state friction model and the LuGre model cause high-frequency oscillations with large amplitudes in velocity, friction force, and pressures, which is not observed in experiments.

Keywords: friction, hydraulic actuator, friction model, simulation, new modified LuGre model

1 Introduction

A hydraulic actuation system is widely used in many applications ranging from robotics and aerospace to mining, construction and underwater manipulators because of its high force/torque and power density. However, the dynamic characteristics of the hydraulic system are relatively complicated due to its high nonlinearities. If the motion of the hydraulic system can be accurately predicted at its design stage by simulation, the design of the system including the selection of the components and the design of the controller will be able to be made appropriately, and the design process may be shortened.

One of the nonlinearities of the hydraulic system is friction. Friction may cause control errors, limit cycles, and poor performance of the system. It is, therefore, necessary to find an accurate mathematical model of friction to predict accurately the motions of the hydraulic system.

Several mathematical models to describe the steady-state friction characteristics have been proposed [1-3] and are widely used in mechanical systems including a hydraulic system. Such steady-state friction models are very useful when steady-state performances of a mechanical system are predicted or analyzed. However, the steady-state friction models are not enough or useless to predict the motion of a hydraulic system, especially for the cases where the system repeats start/stop or inching motion.

Several dynamic friction models have been proposed so far [4-9] and among them, the LuGre model [5] is most widely utilized. The LuGre model, however, cannot simulate well the dynamic friction behaviors of a hydraulic cylinder in the sliding regime as shown in [9]. Yanada and Sekikawa [9] have made a modification to the LuGre model by incorporating lubricant film dynamics into the model and it has been shown that the proposed model, called the modified LuGre model, can simulate the dynamic behaviors of friction observed in hydraulic cylinders with a relatively good accuracy [9-10].

Tran *et al*. [11] have shown that the modified LuGre model is valid only in the negative resistance regime and cannot simulate the hysteretic behaviors observed in hydraulic cylinders in the fluid lubrication regime. In addition, they have revised the modified LuGre model by replacing the usual fluid friction term with a first-order lead dynamics and have shown the usefulness of the new modified LuGre model in the entire sliding regime.

Although the usefulness of the LuGre model and the new modified LuGre model have been verified, the validity of those models in predicting the motion of a hydraulic system has not been investigated.

In this paper, the effect of three friction models, i.e., a steady-state friction model (static + Coloumb + viscous friction), the LuGre model, and the new modified LuGre model on the simulation accuracy of a hydraulic cylinder is examined. Hydraulic cylinder's behaviors such as piston velocity, friction force, and pressures are measured under various operating conditions of sinusoidal input to an electrohydraulic servo valve. Hydraulic cylinder's behaviors are simulated using MATLAB/Simulink by incorporating one of the three friction models with identified parameters into the entire system model. The simulated behaviors are compared with measured ones, and how the simulated behaviors are affected by friction model and which model is the best are discussed.

2 Friction models

In this section, a steady-state friction model, the LuGre model and the new modified LuGre model are described in brief.

2.1 Steady-state friction model

The steady-state friction models that are the combination of Coulomb friction, viscous friction, static friction have been proposed and are summarized in the literature [1,2] and is most commonly used in engineering fields. The friction force is given by a function of velocity as follows:

$$F_r = F_c + (F_s - F_c)e^{-(v/v_s)^n} + \sigma_2 v \tag{1}$$

where F_r is the friction force, F_c is the Coulomb friction and is independent of the magnitude of the velocity, F_s is the static friction force that is observed immediately before there is a slide of the contacting surfaces, v_s is the Stribeck velocity and is related to the velocity range of the negative resistance regime, n is the exponent that affects the slope of the Stribeck curve, σ_2 is the viscous friction coefficient, v is the velocity between the two surfaces in contact. The characteristics of the steady-state friction model are shown in **Fig. 1**.

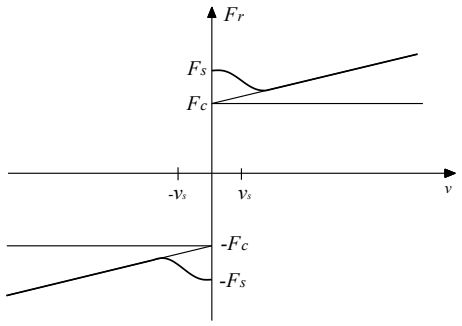

Fig. 1 Steady-state friction model

2.2 LuGre model

Canudas de Wit *et al*. [5] have proposed the LuGre model which combined the stiction behavior with an arbitrary steady-state friction characteristic. The LuGre model is based on the bristle model shown in **Fig. 2**. Contacting asperities on the surfaces are modeled as rigid bristles on one surface and elastic ones on another surface. The LuGre model is given by

$$\frac{dz}{dt} = v - \frac{\sigma_0 z}{g(v)} v \tag{2}$$

$$F_r = \sigma_0 z + \sigma_1 \frac{dz}{dt} + \sigma_2 v \tag{3}$$

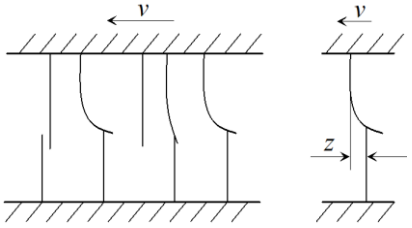

Fig. 2 Bristle model

where z is the mean deflection of the elastic bristles, σ_0 is the stiffness of the elastic bristles, σ_1 is the micro-viscous friction coefficient, $g(v)$ is a Stribeck function given by

$$g(v) = F_c + (F_s - F_c)e^{-(v/v_s)^n} \tag{4}$$

For steady-state, friction force is given by eq. (1).

2.3 New modified LuGre model

Tran *et al.* [11] have extended the modified LuGre model [9] for simulating the dynamic behaviors of friction of hydraulic cylinders in the fluid lubrication regime by replacing the usual fluid friction term with a first-order lead dynamics. The model is called the new modified LuGre model and is described by

$$\frac{dz}{dt} = v - \frac{\sigma_0 z}{g(v,h)} v \tag{5}$$

$$F_r = \sigma_0 z + \sigma_1 \frac{dz}{dt} + \sigma_2 \left(v + T \frac{dv}{dt} \right) \tag{6}$$

where T is the time constant for fluid friction dynamics, $g(v, h)$ is a Stribeck function that expresses the Coulomb friction and the Stribeck effect, and is obtained by incorporating a dimensionless lubricant film thickness, h, into the Stribeck function $g(v)$ of the LuGre model in eq.(4) as follows:

$$g(v, h) = F_c + [(1-h)F_s - F_c]e^{-(v/v_s)^n} \tag{7}$$

The lubricant film dynamics can be given by

$$\frac{dh}{dt} = \frac{1}{\tau_h}(h_{ss} - h) \tag{8}$$

$$\tau_h = \begin{cases} \tau_{hp} & (v \neq 0,\ h \leq h_{ss}) \\ \tau_{hn} & (v \neq 0,\ h > h_{ss}) \\ \tau_{h0} & (v = 0) \end{cases} \tag{9}$$

$$h_{ss} = \begin{cases} K_f \mid v \mid^{2/3} & (|v| \leq |v_b|) \\ K_f \mid v_b \mid^{2/3} & (|v| > |v_b|) \end{cases} \tag{10}$$

$$K_f = (1 - F_c/F_s)|v_b|^{-2/3} \tag{11}$$

where h_{ss} is the dimensionless steady-state lubricant film thickness parameter, K_f is the proportional constant for lubricant film thickness, v_b is the velocity within which the lubricant film thickness is varied, and τ_{hp}, τ_{hn}, τ_{h0} are the time constants for acceleration, deceleration, and dwell periods, respectively. For steady-state, friction force is given by

$$F_{rss} = F_c + [(1 - h_{ss})F_s - F_c]e^{-(v/v_s)^n} + \sigma_2 v \tag{12}$$

In this paper, simulation was done using MATLAB/Simulink. The current supplied to a servo valve was used as the input to the model. The static

parameters of the three models, F_s, F_c, v_s, v_b, n, and σ_2, were identified from the measured steady-state friction characteristics using the least-squares method and the dynamic parameters, σ_0, σ_1, τ_h, and T, were identified by the method proposed in [11].

3 Electrohydraulic servo system and its mathematical model

3.1 Electrohydraulic servo system

The test setup used in this investigation is shown in **Fig. 3**. A single rod (asymmetrical) hydraulic cylinder (2) of which stroke, internal diameter and piston rod diameter are 0.2 m, 0.032 m and 0.018 m, respectively, was fixed vertically on a frame (1) made of U-shape bars and the hydraulic piston was connected to the load mass (5) made of steel circular plates through a rectangular steel plate (4). The motion of the hydraulic piston was controlled by a servo-valve (9). Two pressure sensors (8) with an accuracy of 0.5 %R.O. were used to measure the pressures, P_1, P_2, in the cylinder chambers; the piston velocity, v, was measured using a tacho-generator (6) with a ripple of less than 2% by converting linear motion of the piston to rotational motion through a ball-screw (3) and a belt (7). The ball screw and the tacho-generator were mounted on the frame (1) as shown in **Fig. 3(b)**. Signals from the sensors were read into a computer (10) through a 12-bit analogue-to-digital (A/D) converter and a signal from the computer was supplied to the servo-valve through a 12-bit digital-to-analogue (D/A) converter.

Measured data, i.e., velocity, v, and pressures, P_1, P_2, were recorded at the interval of 0.5 ms (2 kHz). To improve the quality of the measured data, an acausal low-pass filter with a bandwidth of 150 Hz was used to reduce the measurement noise. The acceleration, a, of the piston was calculated by an approximate differentiation of the measured piston velocity. The noise in the calculated acceleration signal was filtered by an acausal low-pass filter with a bandwidth of 32 Hz.

The friction force, F_r, is obtained from the equation of motion of the hydraulic piston using the measured values of the pressures in the cylinder chambers, the acceleration of the piston and the weight of the load mass as follows:

$$F_r = P_1 A_1 - P_2 A_2 - ma - mg \tag{13}$$

where m is the load mass, A_1, A_2 are the piston areas, and g is the acceleration of gravity.

The experiments were conducted at the oil temperature in the oil tank of 30±2 °C and at the supply pressure of P_s=5 MPa under open loop condition. The hydraulic piston is arbitrarily driven by supplying different command inputs of different waveforms. Every experiment was conducted three times to ensure the repeatability.

3.2 Mathematical model

The relationship between the displacement of the valve spool, x_v, and the servo valve control signal, u, can be approximated by a second-order model as follows:

$$x_v = \frac{k_v \omega_v^2}{s^2 + 2\zeta_v \omega_v s + \omega_v^2} u \tag{14}$$

where k_v is the valve spool position gain, ω_v is the valve natural angular frequency and ζ_v is the damping ratio of the servo valve.

The relationship between the volumetric flow rates Q_1, Q_2 and the pressures in both chambers of the cylinder are described in the following forms

$$Q_1 - A_1 \dot{x} = \frac{V_1}{\beta_h} \dot{P}_1 \tag{15}$$

$$A_2 \dot{x} - Q_2 = \frac{V_2}{\beta_h} \dot{P}_2 \tag{16}$$

where β_h is the effective bulk modulus of the fluid, V_1 and V_2 are the total fluid volumes in the two cylinder chambers and are given by

$$V_1 = V_{10} + A_1 x \tag{17}$$

$$V_2 = V_{20} + A_2 (L - x) \tag{18}$$

where L stands for the stroke length of the cylinder and x is the displacement of the mass. V_{10} and V_{20} are the dead volumes in the two cylinder chambers, respectively.

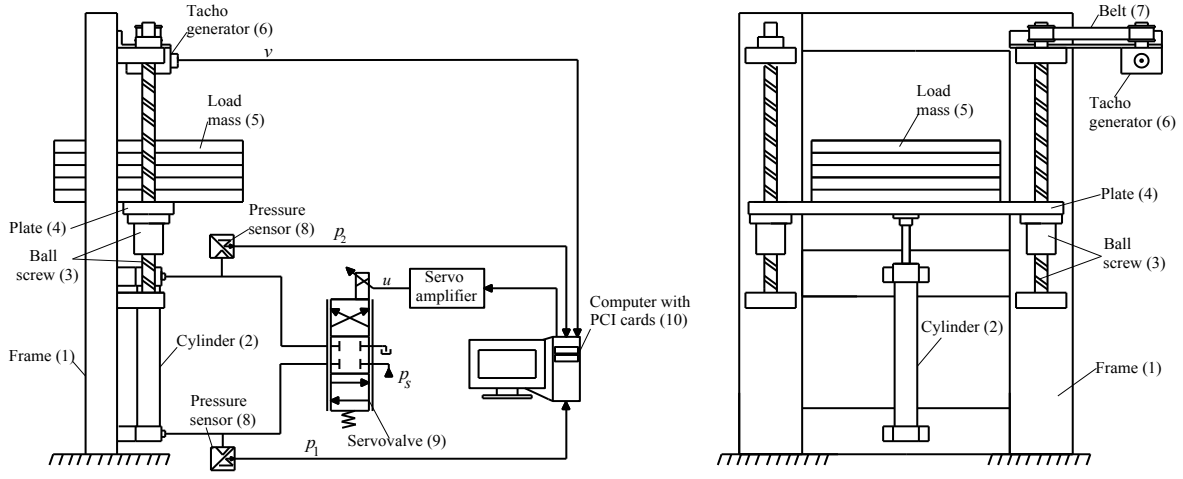

Fig. 3 Schema of experimental apparatus: a) side view b) front view

The volumetric flow rate, Q_1, Q_2, into or out of the chambers 1 and 2 of the cylinder can be written in the following forms:

For $|x_v| \le U$:

$$Q_1 = K_v w(U + x_v)\sqrt{\frac{P_s}{2} + \frac{x_v}{|x_v|}\left(\frac{P_s}{2} - P_1\right)} - K_v w(U - x_v)\sqrt{\frac{P_s}{2} + \frac{x_v}{|x_v|}\left(P_1 - \frac{P_s}{2}\right)} \tag{19}$$

$$Q_2 = K_v w(U + x_v)\sqrt{\frac{P_s}{2} + \frac{x_v}{|x_v|}\left(P_2 - \frac{P_s}{2}\right)} - K_v w(U - x_v)\sqrt{\frac{P_s}{2} + \frac{x_v}{|x_v|}\left(\frac{P_s}{2} - P_2\right)} \tag{20}$$

For $|x_v| > U$:

$$Q_1 = K_v w(U + x_v)\sqrt{\frac{P_s}{2} + \frac{x_v}{|x_v|}\left(\frac{P_s}{2} - P_1\right)} \tag{21}$$

$$Q_2 = K_v w(U + x_v)\sqrt{\frac{P_s}{2} + \frac{x_v}{|x_v|}\left(P_2 - \frac{P_s}{2}\right)} \tag{22}$$

where P_s is the supply pressure to the servo valve and w is the circumferential width of the rectangular port cut into the valve sleeve, and U is the valve underlap. K_v is given by

$$K_v = c_d\sqrt{2/\rho} \tag{23}$$

where c_d is the discharge coefficient of the valve orifice, ρ is the density of the hydraulic fluid. The analysis of hydraulic servo systems of this type is well documented in the literature [12].

The motion of the hydraulic cylinder can be described as follows:

$$m\frac{dv}{dt} = P_1A_1 - P_2A_2 - F_r - mg \tag{24}$$

The system parameters used in the simulation are given in **Table 1**.

Table 1 System parameters

Parameters	Value
k_v [m/A]	0.0227
ω_v [rad/s]	440
ζ_v	0.75
β_h [Pa]	1×10^8
V_{10} [m^3]	5×10^{-6}
V_{20} [m^3]	1×10^{-6}
U [m]	4×10^{-5}
c_d	0.32
ρ [kg/m^3]	862

4 Results and discussion

4.1 Experiment

Figure 4 shows the steady-state friction characteristic of the hydraulic cylinder measured at the load mass of m=118 kg. Positive velocity corresponds to the extending stroke of the piston and negative one to the retracting stroke. It is shown in **Fig. 4** that the steady-state friction characteristic of the hydraulic cylinder is presented by a Stribeck curve as has been shown in [11], and that the friction force is larger in the extending stroke than in the retracting stroke. These asymmetrical friction characteristics come from the asymmetrical structures of the packing material and the hydraulic cylinder.

Figure 5 shows the measured dynamic characteristics of the hydraulic cylinder under a sinusoidal current input to the servo valve at the load mass of 118 kg. The valve current was varied with the amplitude of 4.5 mA

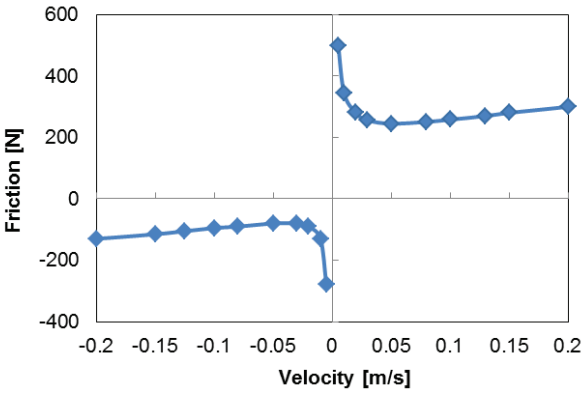

Fig. 4 Steady-state friction characteristic measured at load mass *m* =118 kg

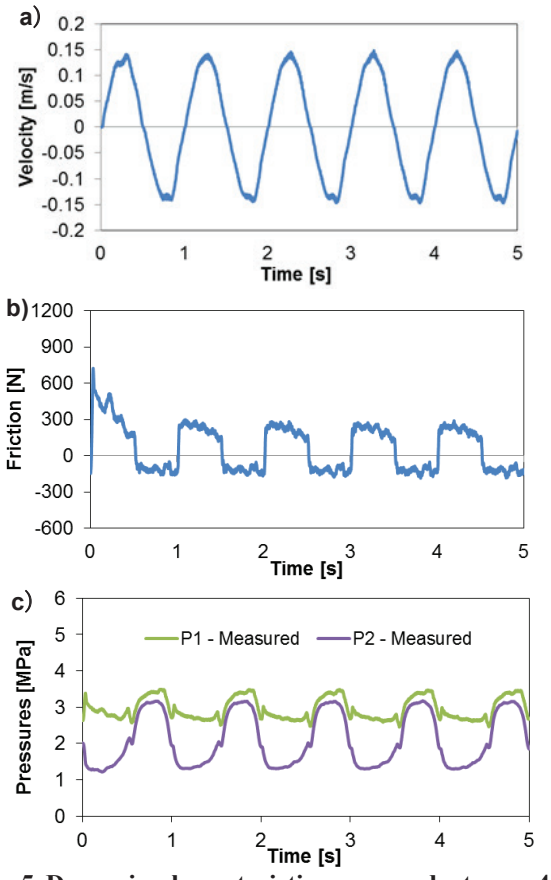

Fig. 5 Dynamic characteristic measured at *u* = 4.5 mA, *f*=1 Hz, *m* =118 kg

and the frequency of 1 Hz. As shown in **Fig. 5**, the friction force, the actuator velocity and the cylinder chamber pressures are strongly interconnected with each other.

The piston velocity variation is shown in **Fig. 5(a)** in which the velocity is varied sinusoidally ranging between -0.14 m/s and +0.14 m/s. **Fig 5(b)** shows that the maximum friction force (break-away force) can be seen instantaneously after starting from the rest. After the friction force has attained its maximum, it decreases continuously in the following period of velocity variation in the first half cycle. After that, the sign of the friction force is reversed almost at the same time as the velocity reversal. After the first cycle of the velocity variation, almost the same friction behavior is repeated. Regarding the pressure variation in **Fig. 5(c)**, it can be noticed that the pressure P_1 is always greater than the pressure P_2 because of the large load mass.

Based on the measured steady-state and dynamic friction characteristics, the parameters of the three models were identified. The identified results of the parameters are shown in **Table 2.**

Table 2 Values of the static parameters of the models

Parameters	$v > 0$	$v > 0$
F_s [N]	830	500
F_c [N]	210	80
v_s [m/s]	0.0125	0.01
v_b [m/s]	0.7	0.9
n	0.05	0.05
σ_2 [Ns/m]	330	350
T [s]	0.33	0.07
σ_0 [N/m]	5×10^6	
σ_1 [Ns/m]	0.1	
τ_{hp} [s]	0.25	
τ_{hn} [s]	1.5	
τ_{h0} [s]	40	

4.2 Simulation

Figure 6 shows comparisons between the dynamic characteristics measured and the ones simulated by the new modified LuGre model at the conditions of u =2mA, f=0.5 Hz and m=118kg. As can be seen from **Fig. 6**, the simulated results of the velocity and the friction force are in good overall agreement with the measured ones. The pressures are not in so good agreement between the simulation and experiment, especially in the negative velocity range, but the overall tendency is similar between both.

Figure 7 shows the comparisons between the dynamic characteristics measured and the ones simulated by the LuGre model. It is shown that the friction force cannot be simulated precisely by the LuGre model as has already been shown [9]. In addition, oscillations are observed in the velocity variation. Such velocity oscillations cause the oscillations of friction force as well as pressures. It is considered that such oscillatory behaviors are caused by large, steep variations in friction force at the velocity reversals.

Figure 8 shows the comparisons between the dynamic characteristics measured and the ones

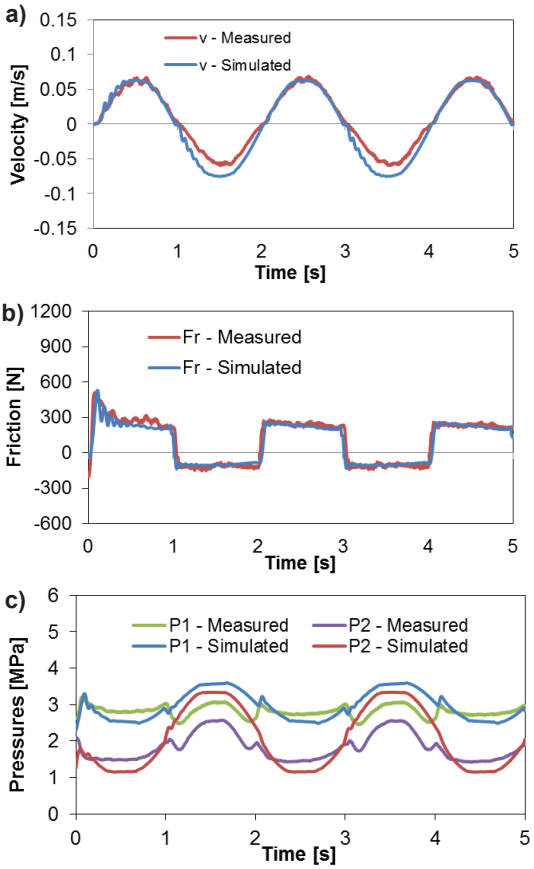

Fig. 6 Comparison between measured and simulated results using the new modified LuGre model at u= 2mA, f=0.5 Hz, m=118 kg

simulated by the steady-state friction model. For this model, the variation of the friction force at velocity reversal becomes larger than that of the LuGre model and because of this, much larger oscillations are seen in the velocity, friction force, and in the pressures. The waveforms of the pressures are almost the same among the three friction models except for the oscillatory components.

5 Conclusions

In this paper, both experiments and simulations are conducted to investigate the effect of friction model on the simulation accuracy of a hydraulic cylinder by using three friction models: a steady-state friction model, the LuGre model, and the new modified LuGre. The results have shown that the new modified LuGre model can predict the hydraulic cylinder's behaviors with a good accuracy. Meanwhile, the steady-state friction model and the LuGre model cannot predict accurately the friction behaviors and cause high-frequency oscillations with large amplitudes in velocity, friction force, and pressures, which are not observed in experiments. In addition, the amplitude of the oscillations is larger for the steady-state friction model than for the LuGre model.

6 Acknowledgement

The authors would like to express their gratitude to Mr. Hiroaki Endo for his help in the simulations.

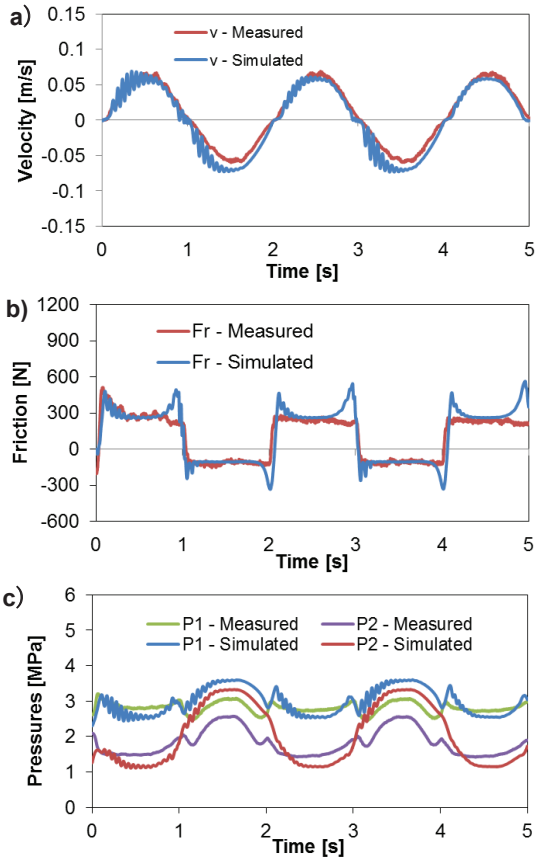

Fig. 7 Comparison between measured and simulated results using the LuGre model at u = 2mA, f=0.5 Hz, m =118 kg

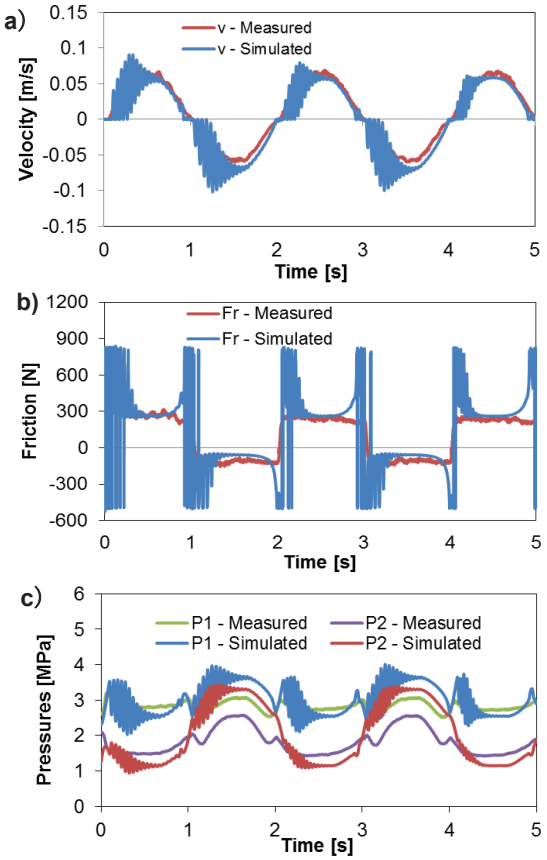

Fig. 8 Comparison between measured and simulated results using the steady-state friction model at u = 2mA, f=0.5 Hz, m =118 kg

References

[1] Armstrong, H. B., "Control of Machines with Friction", Kluwer Academic Publishers, 1991.

[2] Armstrong, H. B., Dupont P., Canudas D. W. C., "A Survey of Models, Analysis Tools and Compensation Methods for the Control of Machines with Friction", Automatica, Vol. 30, No.7, (1994), pp.1083-1138.

[3] Hibi, A., Ichikawa, T., "Mathematical Model of the Torque Characteristics for Hydraulic Motors", Bull. JSME, Vol.20, No.143, (1977), pp.616-621.

[4] Haessig, D. A., Friedland, Jr and B., "On the Modeling of Friction and Simulation", Journal of Dynamic Systems, Measurement, and Control, Vol. 113, No. 3, (1991), pp. 354-362.

[5] Canudas D. W. C., Olsson, H., Åström, K. J., and Linschinsky, P., "A New Model for Control of Systems with Friction", IEEE Transactions on Automatic Control, Vol. 40, No.3, (1995), pp. 419-425.

[6] Dupont P. E. and Dunlop, E. P., "Friction Modeling and PD Compensation at Very Low Velocities", Journal of Dynamic Systems, Measurement, and Control, Vol. 117, No. 1, (1995), pp. 8-14.

[7] Swevers, J., Al-Bencer, F., Ganseman, C. G., and Prajogo, T., "An Integrated Friction Model Structure with Improved Presliding Behavior for Accurate Friction Compensation", IEEE Transactions on Automatic Control, Vol. 45, No. 4, (2000), pp. 675- 686.

[8] Dupont, P., Hayward, V., Armstrong, B., and Altpeter, F., "Single State Elastoplastic Friction Models", IEEE Transactions on Automatic Control, Vol. 47, No. 5, (2002), pp. 787-792.

[9] Yanada, H. and Sekikawa, Y., "Modeling of Dynamic Behaviors of Friction", Mechatronics, Vol. 18, No. 7, (2008), pp. 330-339.

[10] Yanada, H., Takahashi, K., and Matsui, A., "Identification of Dynamic Parameters of Modified LuGre Model and Application to Hydraulic Actuator", Transactions of the Japan Fluid Power System Society, Vol. 40, No. 4, (2009), pp. 57-64.

[11] Tran, X. B., Hafizah, N. and Yanada, H., "Modeling of dynamic friction behaviors of hydraulic cylinders", Mechatronics, Vol. 22, No. 1, (2012), pp. 65-75.

[12] Merrit, H.E., "Hydraulic Control Systems", J.Wiley, 1967.

Received on November 28, 2013
Accepted on February 4, 2014